

AIAA 80-1022R

Analytical Study of the Effects of Wind Tunnel Turbulence on Turbofan Rotor Noise

P. R. Gliebe*

General Electric Company, Cincinnati, Ohio

An analytical study of the effects of wind tunnel turbulence on turbofan rotor noise was carried out to evaluate the effectiveness of the NASA Ames 40×80-ft wind tunnel in simulating flight levels of fan noise. A previously developed theory for predicting rotor/turbulence interaction noise, refined and extended to include first-order effects of inlet turbulence anisotropy, was employed to carry out a parametric study of the effects of fan size, blade number, and operating line for outdoor test stand, NASA Ames wind tunnel, and flight inlet turbulence conditions. A major result of this study is that although wind tunnel rotor/turbulence noise levels are not as low as flight levels, they are substantially lower than the outdoor test stand levels and do not mask other sources of fan noise.

Nomenclature

A	= fan rotor inlet annulus area
AWT1	= Ames wind tunnel, $V_0 = 80$ knots
AWT2	= Ames wind tunnel, $V_0 = 180$ knots
BPF	= blade-passing frequency
C	= contraction ratio
D_t	= fan rotor tip diameter
FLT	= flight, $V_0 = 180$ knots
f	= frequency
f_B	= blade-passing frequency
HF	= high-flow operating line of M_a vs M_t
h	= blade height
LF	= low flow operating line of M_a vs M_t
l_a	= turbulence axial length scale
l_t	= turbulence transverse length scale
M_a	= fan inlet axial Mach number
M_t	= fan inlet tip speed Mach number
M_r	= fan inlet relative Mach number $(M_a^2 + M_t^2)^{1/2}$
N_B	= rotor blade number
N_F	= fan rotative speed, rpm
n	= blade-passing frequency harmonic number
OTS	= outdoor test stand
PR	= fan total pressure ratio
PWL	= acoustic power level, dB re: 10^{-12} W
r	= spanwise radial coordinate
s	= blade-to-blade spacing $2\pi r/N_B$
TCS	= turbulence control structure
U_a	= fan rotor inlet axial velocity
U_t	= fan rotor inlet tip speed
u_a	= axial component of rms turbulence velocity
u_t	= transverse component of rms turbulence velocity
V_0	= wind tunnel velocity or flight speed

Introduction

IT is now well known that acoustic testing of turbofan engines in an outdoor test stand facility does not yield the same noise characteristics as those measured in flight. As discussed in Ref. 1, atmospheric turbulence is drawn into the inlet during ground static testing, undergoing substantial

elongation and contraction. Because of the large contraction of the inflow streamlines, the turbulent eddies convecting with the flow appear as long "sausages" as they pass through the rotor. This is illustrated in Fig. 1. Many blades will successively "chop" the same eddy, producing blade-passing frequency tones as well as broadband noise. This rotor/turbulence interaction is usually strong enough to dominate other sources of fan inlet noise during static testing.

In flight, the fan inlet flow does not undergo very much contraction because of the aircraft forward motion. The fan inlet contraction ratio, defined as fan face through-flow velocity divided by flight speed, is not too different from unity at normal flight approach speeds. At typical approach altitudes (500-1000 ft or 150-300 m), the atmospheric turbulence scales or eddy sizes are much larger than on the ground, so that the eddies do not appear to the rotor as "sausages" which are successively "chopped" by the rotor blades, but may have cross sections as large as, or larger than, the inlet itself. Very little rotor/turbulence interaction noise is therefore produced in flight, allowing other sources to dominate the observed noise spectrum.

It is desirable to have a "static" or ground-based test facility for acoustic evaluation of turbofan engines, one which correctly simulates the flight inlet turbulence conditions. Flight testing is not only costly and time-consuming, but has severe limits on test conditions, power settings, etc., and is subject to variability and uncertainty with respect to atmospheric propagation, ground reflections, and aircraft location. For research and development purposes, extensive hardware changes and elaborate instrumentation and data acquisition equipment are often required which cannot be easily implemented in a flight test. Acoustic testing of full-scale turbofan engines in a large wind tunnel is a viable alternative to flight testing. Flight contraction ratios and aircraft speeds can be simulated in a wind tunnel, under more controlled conditions, with test measurement capability and flexibility rivaling that of a conventional outdoor test stand.

The NASA Ames 40×80-ft wind tunnel facility at Moffett Field, California, has recently been used for acoustic evaluation of turbofan engines under simulated flight conditions. This wind tunnel facility has turbulence properties which are different from both the outdoor test stand and flight altitude environment, and it is important to know whether the rotor/turbulence interaction noise in the tunnel is low enough to provide a true simulation of flight noise characteristics.

The primary objective of the present study was to evaluate the degree to which the NASA Ames 40×80-ft wind tunnel simulates flight conditions in terms of producing sufficiently

Presented as Paper 80-1022 at the AIAA 6th Aeroacoustics Conference, Hartford, Conn., June 4-6, 1980; submitted July 24, 1980; revision received March 23, 1981. Copyright © American Institute of Aeronautics and Astronautics, Inc., 1980. All rights reserved.

*Manager, Aeroacoustic Design Methods Unit, Technical Programs and Performance Technology Department, Aircraft Engine Group. Member AIAA.

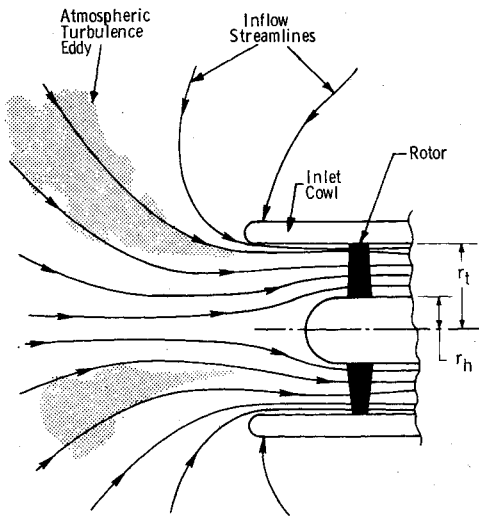


Fig. 1 Fan rotor-turbulence interaction and large-scale turbulent eddy contraction under static test conditions.

M_t = Blade Speed Mach Number
 M_a = Inflow Axial Mach Number

- Fluctuations in M_a Caused by u_a
- Fluctuations in M_t Caused by u_t
- u_a and u_t Produce Fluctuations in Flow Angle α_r

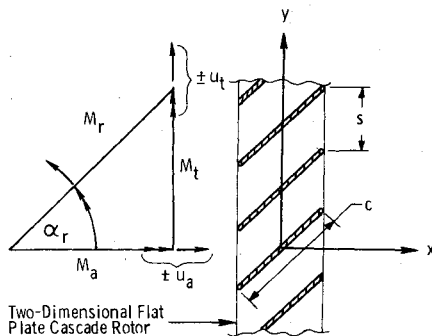


Fig. 2 Rotor-turbulence interaction theory model geometry and nomenclature.

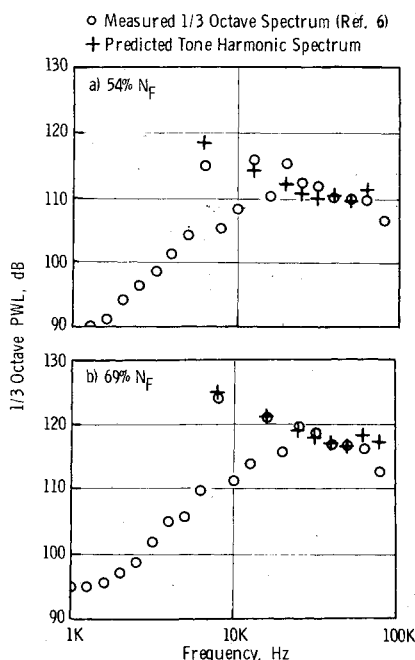


Fig. 3 Predicted vs measured PWL spectrum (inlet arc) for 44-blade scale model fan.

low levels of rotor/turbulence interaction noise. Guidelines for the ranges of fan size, blade number, and operating speeds over which sufficiently low rotor/turbulence noise levels can be expected were to be established. A previously developed theoretical prediction model was to be used for performing the analytical study.

Description and Verification of Theoretical Model

As discussed in Refs. 2 and 3, inlet turbulence may be regarded as a pattern of vorticity convecting with the flow whose statistical properties are known. The nonuniformity of the velocity associated with the turbulence convecting with the flow produces unsteady fluctuations in angle-of-attack on the rotor blades, leading to unsteady blade forces and, hence, noise radiation. This mechanism is usually referred to as a dipole source and is analyzed in detail in Ref. 2.

Further, when the rotor is loaded, i.e., has some steady lift distribution, there is a rotor-locked asymmetric flow pattern spinning in the fan duct having a fundamental period equal to the blade spacing. This asymmetric pattern itself is an ineffective noise source for subsonic tip speeds, but its interaction with inflow turbulence leads to a quadrupole source. The quadrupole source depends on blade loading, whereas the dipole source, to first order, does not. The quadrupole mechanism is treated in detail in Ref. 3.

Based on the above physical picture of noise generation due to turbulence incident on a blade row, theoretical analyses were developed (Refs. 2 and 3) relating the characteristics of the turbulence, design parameters of the blade row, and the spectrum of the radiated noise. A spectral representation of turbulence which treats the turbulence as a superposition of shear waves was used. The turbulence was assumed to be homogeneous and isotropic. The effects of inlet contraction were subsequently accounted for by utilizing sudden-contraction theory,⁴ as illustrated in Fig. 1.

A two-dimensional cascade representation of the blade row is employed, and the blades are idealized as flat plates. The flow is assumed to enter the inlet axially with axial Mach number M_a , while the cascade translates with transverse Mach number M_t , as illustrated in Fig. 2. The turbulence is treated as a superposition of shear waves of varying wavenumber in the axial (x), transverse (y), and spanwise (z) directions.

The computer code utilized herein for the prediction of rotor/turbulence interaction noise is essentially a modified form of the code presented in Ref. 3. The incompressible lift response function (Sears' function) has been replaced by compressible response functions^{5,6} and the inlet contraction effects⁴ have also been added. The anisotropic (axisymmetric) turbulence spectrum model has been added as described in Ref. 7. A simplified formulation which invokes a long length-scale assumption was shown to predict trends quite well in Ref. 7, and this simplified version was used in the parametric studies to follow.

The above-described computer code predicts inlet and exhaust radiated acoustic power (PWL) in narrowband peaks at blade-passing frequency and its harmonics. Input required is M_a , M_t , rotor solidity (defined as chord c over blade spacing s), inlet axial and transverse turbulence intensity, axial and transverse length scales, and inlet contraction ratio. Output includes dipole, quadrupole, and total PWL for both inlet and exhaust ducts.

Noise predictions are made using the rotor blade geometric properties and mean flow conditions at the rms radius of the inlet annulus.

Computed and measured inlet PWL spectra are shown in Fig. 3 for a 44-blade fan stage described in Ref. 8. It can be seen that the prediction of blade-passing frequency tones and harmonics is in good agreement with the data for the new axisymmetric turbulence formulation. It was observed that the theory overpredicts the noise at high frequencies if the relative Mach number is rather high, $M_t > 0.85$ at the pitchline.

Table 1 Summary of typical average inlet turbulence properties for various turbofan engine test facilities ($U_a \sim 122 \text{ m/s}$)

Parameter	Outdoor test stand (static)	NASA Ames $40 \times 80\text{-ft}$ wind tunnel		Aircraft installation ($V_0 = 180 \text{ knots}$)
		$V_0 = 80 \text{ knots}$	$V_0 = 180 \text{ knots}$	
Location	Fan face	Upstream	Upstream	Upstream
$u_a, \text{m/s}$	1.2	0.081	0.183	1.4
$u_t, \text{m/s}$	4.8	0.224	0.503	1.4
l_a, m	30.5	0.414	1.83	91-213
l_t, m	0.12	N/A	N/A	91-213
$C = U_a/V_0$	40-50	3.0	1.33	1.33

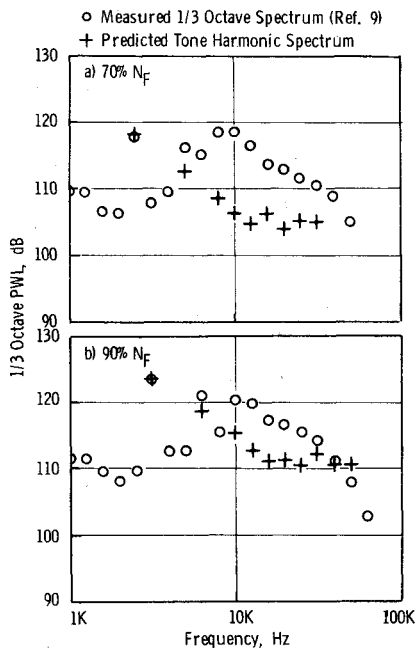


Fig. 4 Predicted vs measured PWL spectrum (inlet arc) for 18-blade variable pitch scale model fan.

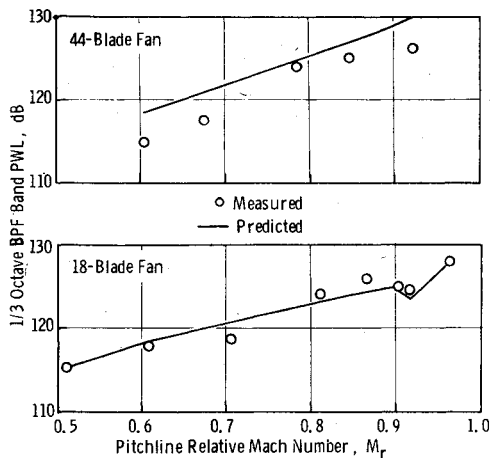


Fig. 5 Predicted vs measured BPF tone level as a function of M_r for scale model fans.

Data/theory comparisons were also carried out for a scale model 18-blade variable-pitch fan tested in the same anechoic chamber as was the 44-blade fan stage reported in Ref. 8. Inlet arc $\frac{1}{3}$ -octave PWL spectrum comparisons are shown in Fig. 4, the data being taken from Ref. 9. The BPF tones are predicted quite well for both fans, except at transonic relative Mach numbers, as shown in Fig. 5.

To test the ability of the prediction model to evaluate wind tunnel turbulence noise for a fan, predictions were made of the BPF tone PWL (inlet arc) for the 15-blade fan tested in the NASA Lewis $9 \times 15\text{-ft}$ wind tunnel, the results of which are

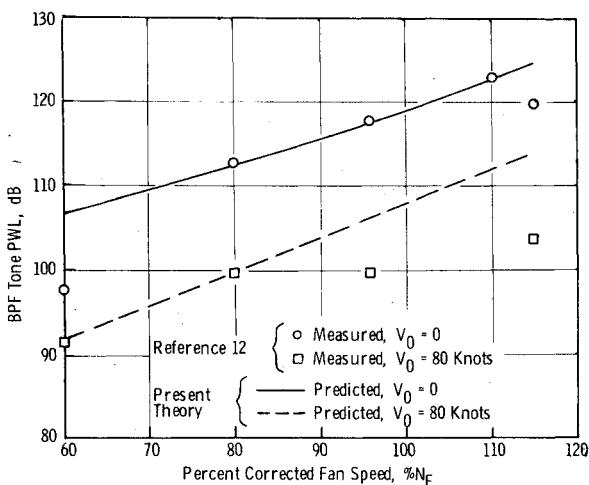


Fig. 6 Predicted vs measured BPF tone PWL for rotor 55 in NASA Lewis $9 \times 15\text{-ft}$ wind tunnel (Ref. 12).

given in Ref. 10. In this case, turbulence measurements were made inside the fan duct close to the rotor. For the static ($V_0 = 0$) case, the measured transverse and axial intensities were used to estimate the effective contraction ratio, using the sudden-contraction theory, and this contraction ratio was used to estimate the *transverse length scale only*, based on measured axial length scale. For the wind-on case, $V_0 = 80$ knots, the actual contraction U_a/V_0 was used to estimate the transverse length scale.

The resulting predictions of BPF tone PWL vs fan speed for both static and wind-on conditions is shown in Fig. 6 along with the measured values. It can be seen that the agreement is, on the average, reasonably good, considering the approximations and assumptions made, lending further support to the validity of the basic rotor/turbulence interaction prediction model.

Based on the analysis and review of existing data described above, the current rotor/turbulence interaction noise model appears to be adequate for predicting wind-tunnel turbulence/rotor interaction noise when the fan face turbulence properties are known.

Parametric Studies

Inlet Turbulence Properties

A literature survey of published data on fan inlet turbulence properties was carried out. From this survey, an "expected ensemble average" set of turbulence properties was deduced for a typical outdoor test stand and the NASA Ames $40 \times 80\text{-ft}$ wind tunnel. Expected average values for in-flight conditions were derived from the results of flight test correlations of atmospheric turbulence summarized by Houbolt.¹¹

A table of typical expected values of inlet turbulence velocities and scales are given in Table 1. The outdoor test stand expected values are weighted heavily by the data of Hanson,^{1,12} as well as previously unpublished data taken on a fan engine at the General Electric Company, Peebles, Ohio, test facility.

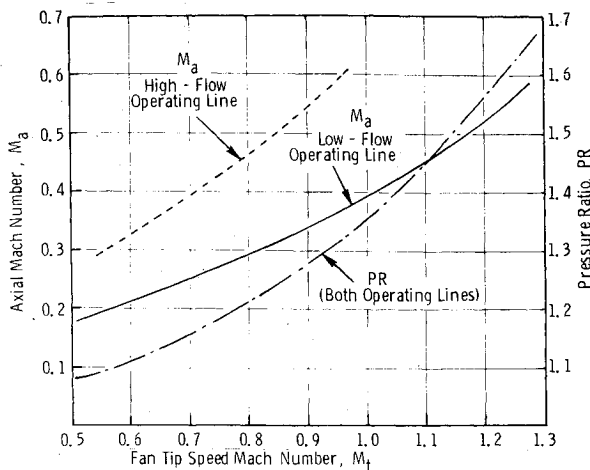


Fig. 7 Axial Mach number vs tip speed Mach number and pressure ratio vs tip speed Mach number for typical fan stages.

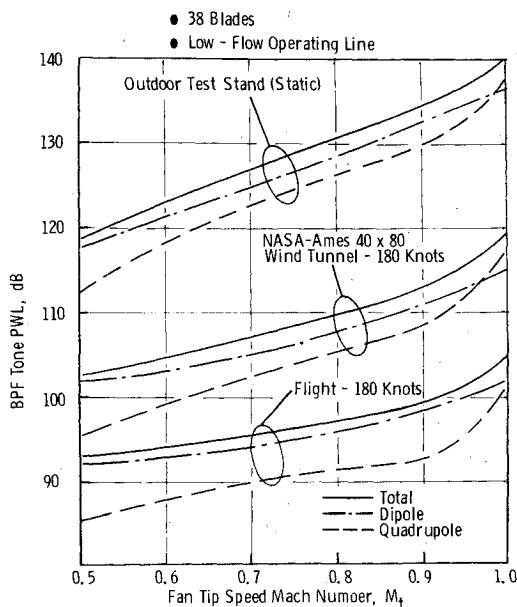


Fig. 8 Component source contributions to BPF tone PWL for full-scale fans with different inlet conditions.

For the flight case, no fan inlet measurements of turbulence were available. However, the atmospheric properties can be used¹¹ along with contraction ratio corrections as outlined in Ref. 4. The contraction ratio is assumed to be equal to the fan face axial velocity divided by flight velocity, i.e., $C = U_a/V_0$.

The NASA Ames 40×80-ft wind tunnel properties are taken from Ref. 13. The measurements were made 20 ft upstream of the fan inlet, and no fan face measurements were available. Both tangential and axial turbulence velocities are given, but only axial length scale was measured. Hence the transverse length scale must be deduced from the ratio of tangential to axial turbulence velocity and the sudden contraction theory.⁴ This amounts to assuming that somewhere upstream of the measurement point the turbulence was isotropic, and that the eddy elongation and cross section contraction correspond to the measured velocity ratio. The turbulence at the measuring point is assumed to undergo another "sudden" contraction from the measuring point to the fan face, and the relations developed in Ref. 4 are used to compute the fan face spectra from the measuring point spectra. The contraction ratio in this case is assumed to be the ratio of fan face velocity to tunnel velocity, $C = U_a/V_0$.

Fan Geometry and Operating Line

The prediction program requires as input the fan rotor inlet axial and rotational Mach numbers and rotor total pressure ratio. A composite plot of these fan parameters was made for

several fan stages, including those discussed in the previous section. Many of the fans have a common flow vs speed (M_a vs M_t) characteristic, and a common work vs speed (PR vs M_t) characteristic. A common operating characteristic of M_a and PR vs M_t was therefore selected for the parametric study, and these are shown in Fig. 7. This is henceforth referred to as the low-flow (LF) transonic fan operating line. The variable-pitch fan and NASA 15-blade fans, however, have higher M_a vs M_t characteristics (dashed line in Fig. 7), and this is related to their design tip speeds, which are subsonic. A limited number of calculations was therefore performed using this flow characteristic (M_a vs M_t), and this operating line is henceforth referred to as the high-flow (HF) subsonic fan characteristic.

Several fan sizes were selected for study because it is known from theoretical considerations that the turbulence scale-to-blade spacing ratio is important. Hence different fan sizes operating in the same turbulence environment may give different noise levels when the levels are corrected to a common fan inlet area. Fan diameters of 2.13 m (84 in.), 1.07 m (42 in.), and 0.53 m (21 in.) were selected for study.

Blade number was also varied, values of $N_B = 38, 28$, and 18 being selected for study. These values represent the range of fan types currently in use. For example the diameter/blade number combination 2.13 m/38 is close to the GE CF6 engine fan, and the combination 0.53 m/28 is similar to the P&WA JT15D engine fan.

Blade tip solidity was held constant at $(c/s)_{tip} = 1.3$ for all LF transonic fan cases and 1.0 for all HF subsonic fan cases, as it is usual design practice to set rotor tip solidity approximately equal to design tip relative Mach number.

Calculations of rotor/turbulence noise were made for each of the above configurations, over the tip speed Mach number range $0.5 < M_t < 1.0$. The calculations were performed for several turbulence conditions, as follows: 1) Outdoor test stand (OTS), 2) Ames 40×80-ft wind tunnel, $V_0 = 80$ knots (AWT1), 3) Ames 40×80-ft wind tunnel, $V_0 = 180$ knots (AWT2), 4) In-flight, $V_0 = 180$ knots (FLT).

Noise levels were obtained at blade-passing harmonics $n = 1-8$ for all cases. Some parametric studies were also made of the effect of length scale and flight speed.

Component Source Contributions

The relative contributions of the dipole (unsteady lift) and quadrupole (steady loading/turbulence interaction) sources to the total predicted rotor/turbulence noise were examined first. Figure 8 shows typical contributions for the full-scale (2.13 m diam) fans on the low-flow operating line. Note that the dipole source dominates the BPF tone. Sample spectra, i.e., tone PWL vs harmonic number n , showing dipole and quadrupole contributions, are given in Fig. 9.

It was observed from these and other results that the trends of BPF tone PWL with Mach number M_t are similar for OTS and AWT, but the FLT condition yields a flatter curve. Also, the quadrupole contribution, for the FLT condition is not as great as in the other test site conditions. Even though the BPF tone levels in the AWT are similar at $V_0 = 80$ and 180 knots, the higher harmonics of BPF are 2-5 dB lower at 180 knots relative to levels at 80 knots, the larger differences occurring at the higher tip speed Mach numbers.

Effect of Blade Number

The higher harmonics of BPF decrease with increasing blade number, even though the effect of blade number is very small at BPF. The effect of blade number is shown explicitly in Fig. 10. Increasing the number of blades for a given solidity decreases the blade spacing and hence increases the tangential length scale-to-blade spacing parameter, l_t/s , resulting in a noise reduction. However, increasing the number of blades N_B also increases rotor blade aspect ratio, resulting in a higher unsteady lift amplitude. The dipole noise therefore increases, off-setting the decrease due to increasing l_t/s . But the dipole source only dominates at BPF, so the net result is little or no change in noise with N_B at BPF but decreasing

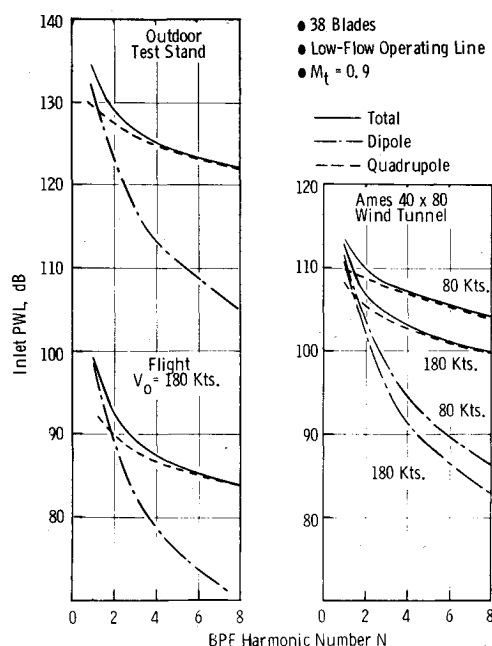


Fig. 9 Contribution of dipole and quadrupole sources to PWL harmonic spectrum.

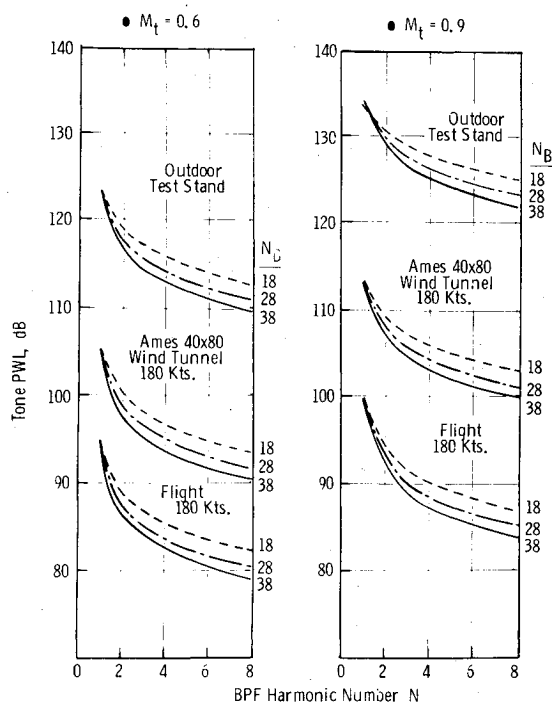


Fig. 10 Effect of blade number on harmonic spectrum for full-scale fan on low-flow operating line.

noise with increasing N_B at second harmonic ($n=2$) and higher frequencies.

Effect of Fan Size

To show explicitly the effect of fan size, some of the predictions were normalized with respect to fan rotor inlet area by subtracting $10 \log_{10} (A/A_{ref})$ from predicted noise levels, where A_{ref} is a reference area, taken arbitrarily to be 1 m^2 . The tone PWL results normalized in this fashion are shown in Fig. 11. The major observation to be made is that size does make a difference, i.e., *rotor/turbulence noise does not scale with fan area unless the turbulence scales are changed in proportion to the fan diameter change.*

The results shown in Fig. 11 show that the smaller fans yield less noise than the area reduction effect can account for, by 5-10 dB. This again is related to the difference in l_t/s which

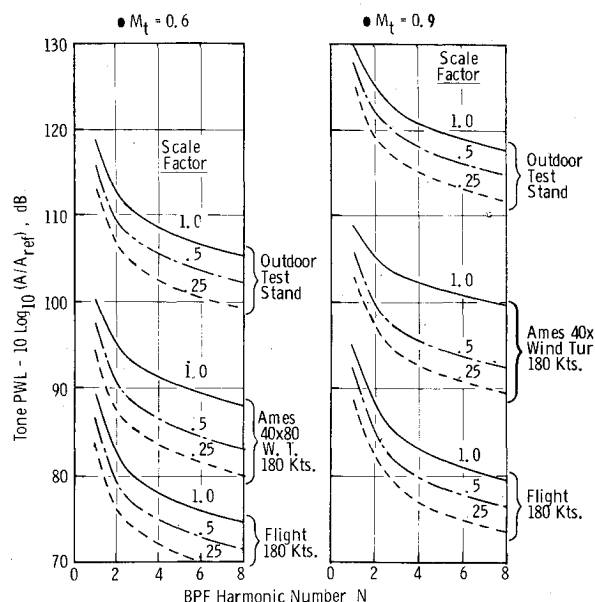


Fig. 11 Effect of fan size on tone PWL spectrum for 38-blade fans on low-flow operating line.

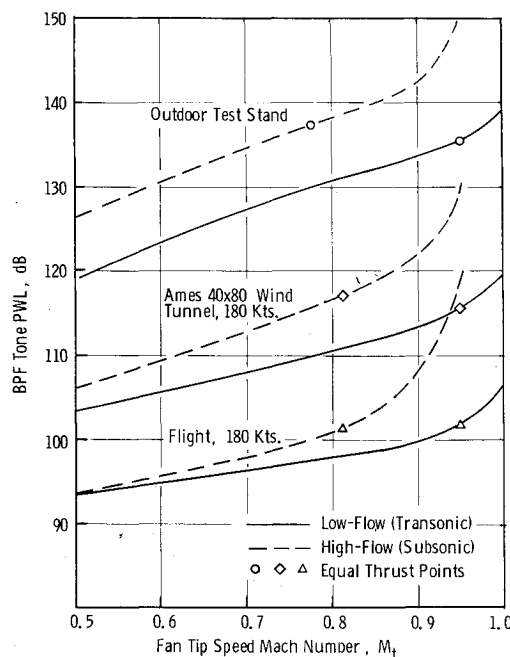


Fig. 12 Effect of operating line on BPF tone PWL for full-scale 18-blade fans.

occurs because the turbulence scales (l_t) remain the same while the geometric scales (s) decrease with decreasing fan size.

Effect of Operating Line

Comparisons were made of rotor/turbulence noise of full-scale fans with 18 blades for two operating lines: 1) the low-flow (LF) line of Fig. 7 for typical high tip speed fans, and 2) the high-flow (HF) operating line of Fig. 7 for typical subsonic tip speed fans such as the variable-pitch fan. The BPF tone PWL comparisons are shown in Fig. 12. It is seen from these results that, at a given tip speed Mach number, the HF fan is noisier than the LF fan.

The higher inlet relative Mach number for the high-flow fan is responsible for some of the noise differences shown in Fig. 12. Assuming the noise to be proportional to M_t^6 , a 3 dB higher noise level would be expected for the HF fan based on Mach number level differences alone. The aspect ratio for the HF fan is higher because of the lower tip solidity, and unsteady lift is therefore higher for the HF fan. The aspect ratio

effect alone is estimated to be 3.0-3.7 dB for this case. These effects account for most all of the differences shown in Fig. 12 for the outdoor test stand.

For the Ames wind tunnel and flight conditions, however, the higher axial Mach number for the HF fan gives a larger contraction ratio at a given tip speed. This has the effect of reducing the tangential length scale (l_t/s), which increases the noise. However, it is also in the direction of reducing turbulence intensity at the fan face, which decreases the noise. The latter effect apparently overshadows the decreased-scale effect, since the HF fan and LF fan noise levels are nearly the same at low tip speeds. The rapid divergence near $M_t=0.9$ between the two operating-line curves is due to the fact that for the HF fan the rotor inlet relative Mach number is approaching unity at these high speeds, causing the quadrupole source contributions to become disproportionately high as they approach their singularity points.

The HF fan will produce more propulsive thrust at a given tip speed than the LF fan, because the flow is higher and the pressure ratio is the same. It is therefore of interest to compare the HF fan with the LF fan at the same net thrust. These equivalent thrust points are indicated on Fig. 12 by symbols for a typical LF fan approach power tip speed Mach number of $M_t=0.95$. It can be seen that the HF fan and LF fan rotor/turbulence noise levels are approximately the same at the same thrust.

NASA Ames 40 × 80-Ft Wind Tunnel Evaluation

Based on the results of the parametric study discussed in the preceding section, an evaluation of the NASA Ames 40 × 80-ft wind tunnel was carried out to assess the range of fan geometries, operating speeds, and tunnel speeds over which the Ames tunnel adequately simulates flight conditions as far as rotor/turbulence noise is concerned. The objective was to define the operational/geometric boundaries for adequate flight simulation.

Before carrying out the evaluation, an assessment of the wind-tunnel rotor/turbulence noise prediction level variability was made to establish an uncertainty band in predicted levels. There is an uncertainty associated with taking turbulence properties measured 8-10 fan diam upstream of the engine and projecting these to fan rotor inlet values using sudden-contraction theory. One extreme is to assume that the sudden-contraction theory is correct, which qualitatively gives

$$(u_a/U_a)_{\text{fan}} \sim (u_a/V_0)_{\text{tunnel}} C^{-2}$$

and

$$(u_t/U_a)_{\text{fan}} \sim (u_t/V_0)_{\text{tunnel}} C^{-1/2}$$

Thus both axial and transverse intensities are lower after the contraction. This assumption gives the lower bound in noise predictions. The other extreme is to assume that the intensities do not change at all across the contraction so that

$$(u_a/U_a)_{\text{fan}} \sim (u_a/V_0)_{\text{tunnel}}$$

and

$$(u_t/U_a)_{\text{fan}} \sim (u_t/V_0)_{\text{tunnel}}$$

This gives an upper bound on the noise predictions. Now across a contraction, u_a will decrease by some amount and u_t will increase. In any case, u_t will be substantially larger than u_a , and hence the noise level will be primarily governed by the variations in u_t and variations in u_a will have little or no effect. An estimate of the difference between the upper and lower bound limits can therefore be made by noting² that the noise varies as the square of the turbulence intensity. Defining ΔPWL as the difference between upper and lower bound predictions, where subscripts A and B refer to precontraction and postcontraction values, we can assume that

$$\Delta\text{PWL} \approx -20 \log_{10} \{ [(u_t)_B/U_a] / [(u_t)_A/V_0] \}$$

The numerator represents the lower bound value of transverse intensity at the fan face given by sudden contraction theory, while the denominator represents the upper bound value corresponding to no change in intensity. This equation was used to estimate the difference in calculated noise levels between the above two assumptions concerning contraction effects.

The uncertainty band due to contraction effects is about 2 to 6 dB at $V_0=80$ knots over a range of tip speeds $0.5 < M_t < 1.0$. At 180 knots the uncertainty band is only 0 to 2 dB for the tip speed range $0.75 < M_t < 1.0$. For $M_t < 0.75$ at $V_0=180$ knots, the contraction ratio is less than 1.0, i.e., $V_0 > U_a$, and applicability of contraction theory to expanding flows is questionable.

It is emphasized that the above uncertainty band is not due to variability and/or randomness in the tunnel turbulence properties, but is only due to the uncertainty in the techniques being used to extrapolate that turbulence information to the fan face values. In fact, the same uncertainty applies to the flight case, because upstream atmospheric turbulence characteristics are being extrapolated to fan face values with the same techniques. Also the maximum (6 dB) uncertainty band is less than the tone fluctuation amplitudes usually observed for rotor/turbulence noise.¹⁰

The outdoor test stand predictions also have an uncertainty band due to the variability in turbulence properties which are measured at the fan face. For example, measured axial length scales varied from 26 to 79 m (86 to 259 ft) at the GE Peebles, Ohio test facility for one engine test. From these results, it was concluded that an uncertainty of +1 to -4 dB can exist in predicted outdoor test stand levels due to uncertainty in knowing axial length scale, recalling that a nominal value of $l_a=30.5$ m (100 ft) was used for all OTS calculations discussed in the previous section. Also, the measured transverse intensity u_t/U_a varied by a factor of 2, implying an additional ± 3 dB uncertainty due to variability in u_t/U_a .

Finally, the uncertainty in predicted flight rotor/turbulence noise levels must be considered. Houbolt¹¹ quotes many data sources, and suggests that a rather alarming variability in atmospheric turbulence conditions can prevail, depending upon the proximity of weather fronts, wind shear, squall lines, thunderstorms, temperature gradients, terrain, etc. Aircraft wake turbulence in the vicinity of airports will introduce variations dependent upon traffic patterns, density, and duration. Houbolt estimates the variation in atmospheric turbulence length scales to be from 91 to 213 m (300 to 700 ft). A nominal value of 152 m (500 ft) was used in the present study. It was estimated that the uncertainty in predicted noise levels for the length scale range of 91 to 213 m is about ± 2 dB. Houbolt also states that atmospheric turbulence rms velocities of 3.0-3.5 ft/s are average values, with possible peak "gust" values of 20 times as much. Such extremes are rare and are confined to severe weather conditions, but nevertheless highlight the variability that can be expected in rotor/turbulence noise in flight. A 4:1 variation in precontraction u_t is not unreasonable in flight, which would then yield a ± 6 dB variation in noise. Combined with the ± 2 dB uncertainty due to variations in length scale, a total uncertainty band on predicted flight rotor/turbulence noise levels of ± 8 dB is the best that can be expected, based on atmospheric turbulence variability from the "expected average" values.

From the results summarized in Figs. 8-12, rotor/turbulence noise levels in the Ames 40 × 80-ft wind tunnel are predicted to be 15-20 dB lower, on the average, than the OTS levels, but still about 10-15 dB higher than corresponding flight levels. The question that arises is, are the wind tunnel levels low enough? To answer this, first recall that the noise level increases with decreasing blade number, and that full-scale fans produce more "noise-per-unit-area" than do scale model fans. If we take into account all of the above uncertainty band limits and consider as the worst case the full-

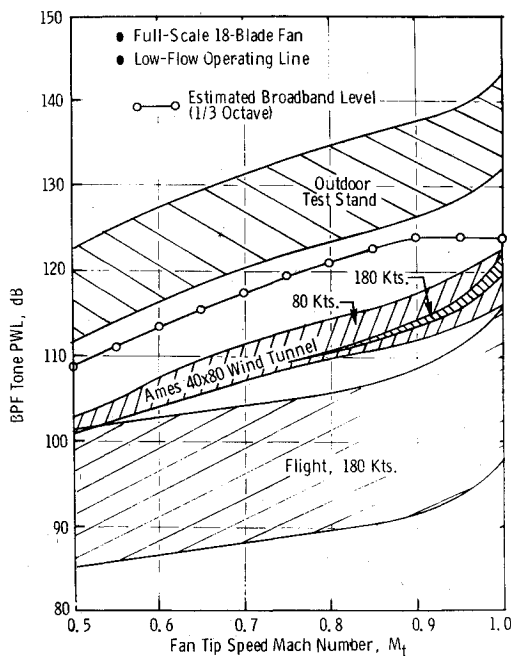


Fig. 13 Predicted variability in rotor-turbulence noise BPF tone PWL due to variations and uncertainties in fan face turbulence levels.

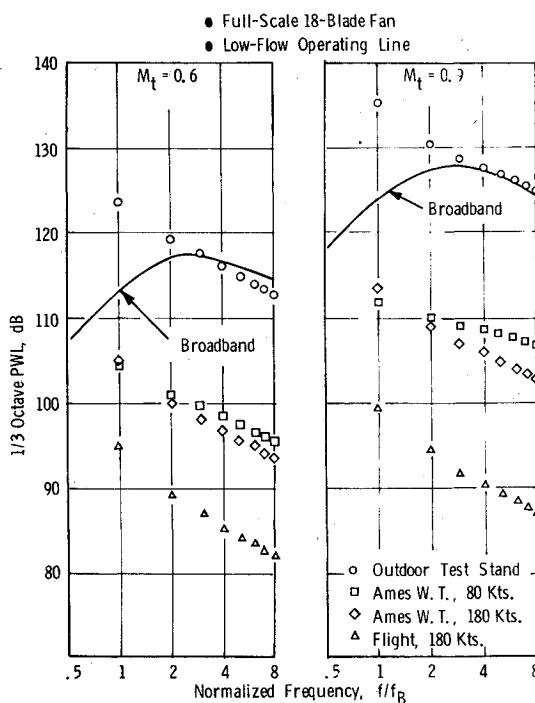


Fig. 14 Comparison of rotor-turbulence tone levels with fan $1/3$ -octave broadband spectrum.

scale 18-blade fan, the comparison of predicted BPF tone levels for the various test conditions would look more like Fig. 13, where a band or range of values is shown rather than a single average line. The point to be learned from this figure is that when variability is taken into account, the wind tunnel levels can be as low as flight levels, even though the average line predictions show a 10-15 dB difference. Also, the uncertainty band associated with variability in turbulence properties for the OTS and flight conditions is considerably larger than the uncertainty for the Ames 40×80 -ft wind tunnel due to extrapolating upstream turbulence characteristics to the fan face conditions.

Another way of assessing the adequacy of the NASA Ames 40×80 -ft tunnel for simulating flight turbulence levels is to see how much tone reduction is obtained relative to the fan

characteristic broadband level. An empirical method for correlating fan broadband noise was published in Ref. 14, and this method was used to correlate the broadband levels of several scale model fan stages, using data with a turbulence control structure in place (Ref. 8). The correlations, given in Ref. 15, relate the peak broadband level to rotor inlet tip relative Mach number M_r and rotor tip incidence angle (relative air angle minus blade leading edge camberline angle). This correlation was used to estimate the broadband level ($1/3$ octave) at the blade-passing frequency, and these results are also shown in Fig. 13. It can be seen that the NASA Ames 40×80 -ft wind tunnel rotor/turbulence tones are well below the predicted broadband levels at all but the highest tip speeds.

The spectral distribution of the rotor/turbulence tones is shown in Fig. 14, compared with predicted $1/3$ -octave fan broadband noise spectra. It is apparent from this comparison that the higher harmonics of BPF rotor/turbulence tones are well below the fan broadband noise level for the Ames 40×80 -ft wind tunnel case. Additional higher harmonic tone sources (i.e., rotor-stator interaction noise) will no doubt dominate the spectrum.

Conclusions

In summary, based on all the calculations and parametric studies discussed herein, it is concluded that the NASA Ames 40×80 -ft wind tunnel provides adequate suppression (or reduction) of rotor/turbulence noise such that proper simulation of flight fan source noise characteristics is obtained, for subsonic tip speeds. Near M_r approaching unity, wind tunnel rotor/turbulence tones may be as high as or higher than the broadband level, but cut-on of the rotor-alone noise field at $M_r = 1$ will probably mask this effect.

Acknowledgments

The work described herein was supported by NASA Ames Research Center under Contract NAS2-10002, monitored by Warren Ahtye. The author gratefully acknowledges the NASA Ames Research Center and the General Electric Company for granting permission to publish this study. The author also gratefully acknowledges the encouragement, advice, and guidance provided by E.B. Smith and M.T. Moore of the General Electric Company, and the stimulating discussions held with C. Feiler, J. Groneweg, and L. Shaw of NASA Lewis Research Center on the subject of wind tunnel turbulence contraction effects.

References

- Hanson, D.B., "Spectrum of Rotor Noise Caused by Atmospheric Turbulence," *Journal of the Acoustical Society of America*, Vol. 6, No. 1, July 1974.
- Mani, R., "Noise Due to Interaction of Inlet Turbulence with Isolated Stators and Rotors," *Journal of Sound and Vibration*, Vol. 17, No. 2, 1971, pp. 251-260.
- Mani, R., "Isolated Rotor Noise Due to Inlet Distortion or Turbulence," NASA Contractor Report 2479, Oct. 1974.
- Ribner, H.S. and Tucker, M., "Spectrum of Turbulence in a Contracting Stream," NASA Report 1113, 1953.
- Osborne, C., "Unsteady Thin-Airfoil Theory for Subsonic Flow," *AIAA Journal*, Vol. 11, No. 2, Feb. 1973, pp. 205-209.
- Amiet, R.K., "High-Frequency Thin-Airfoil Theory for Subsonic Flow," *AIAA Journal*, Vol. 14, No. 8, Aug. 1976, pp. 1076-1082.
- Kerschen, E.J. and Gliebe, P.R., "Fan Noise Caused by Ingestion of Anisotropic Turbulence—A Model Based on Axisymmetric Turbulence Theory," AIAA Paper 80-1021, AIAA 6th Aeroacoustics Conference, Hartford, Conn., June 1980.
- Kantola, R.A. and Warren, R.E., "Basic Research in Fan Source Noise—Inlet Distortion and Turbulence Noise," NASA Contractor Report 149451, Dec. 1978.
- Bilwakesh, K.R., Clemons, A., and Stimpert, D.L., "Quiet Clean Short-Haul Experimental Engine (QCSEE) Acoustic Performance of a 50.8 cm (20-inch) Diameter Variable-Pitch Fan and Inlet, Test Results and Analysis, Vol. 1," NASA CR-135177, April 1979.

¹⁰Shaw, L.M., Woodward, R.P., Glaser, F.W., and Dastoli, B.J., "Inlet Turbulence and Fan Noise Measured in an Anechoic Wind Tunnel and Statically With an Inlet Flow Control Device," AIAA Paper 77-1345, AIAA 4th Aeroacoustics Conference, Atlanta, Ga., Oct. 1977.

¹¹Houbolt, J.C., "Atmospheric Turbulence," *AIAA Journal*, Vol. 11, No. 4, April 1973, pp. 421-437.

¹²Hanson, D.B., "Measurements of Static Inlet Turbulence," AIAA Paper 75-467, AIAA 2nd Aeroacoustics Conference, Hampton, Va., March 1975.

¹³Hodder, B.K., "40- \times 80-Foot Wind Tunnel Free-Stream Turbulence Measurements," NASA Ames FSA Technical Memorandum 17, April 1977.

¹⁴Ginder, R.B. and Newby, D.R., "An Improved Correlation for the Broadband Noise of High Speed Fans," *Journal of Aircraft*, Vol. 14, No. 9, Sept. 1977, pp. 844-849.

¹⁵Gliebe, P.R., "The Effect of Throttling on Forward Radiated Fan Noise," AIAA Paper 79-640, AIAA 5th Aeroacoustics Conference, Seattle, Wash., March 1979.

From the AIAA Progress in Astronautics and Aeronautics Series . . .

INJECTION AND MIXING IN TURBULENT FLOW—v. 68

By Joseph A. Schetz, Virginia Polytechnic Institute and State University

Turbulent flows involving injection and mixing occur in many engineering situations and in a variety of natural phenomena. Liquid or gaseous fuel injection in jet and rocket engines is of concern to the aerospace engineer; the mechanical engineer must estimate the mixing zone produced by the injection of condenser cooling water into a waterway; the chemical engineer is interested in process mixers and reactors; the civil engineer is involved with the dispersion of pollutants in the atmosphere; and oceanographers and meteorologists are concerned with mixing of fluid masses on a large scale. These are but a few examples of specific physical cases that are encompassed within the scope of this book. The volume is organized to provide a detailed coverage of both the available experimental data and the theoretical prediction methods in current use. The case of a single jet in a coaxial stream is used as a baseline case, and the effects of axial pressure gradient, self-propulsion, swirl, two-phase mixtures, three-dimensional geometry, transverse injection, buoyancy forces, and viscous-inviscid interaction are discussed as variations on the baseline case.

200 pp., 6 \times 9, illus., \$17.00 Mem., \$27.00 List

TO ORDER WRITE: Publications Dept., AIAA, 1290 Avenue of the Americas, New York, N. Y. 10019